

Photovoltaic-thermal (*PV/t*) panel to minimize electrical and air conditioning energy consumption of a typical office in Beirut

S. Makarem, K. Ghali, N. Ghaddar & S. Karaki

To cite this article: S. Makarem, K. Ghali, N. Ghaddar & S. Karaki (2016) Photovoltaic-thermal (*PV/t*) panel to minimize electrical and air conditioning energy consumption of a typical office in Beirut, *International Journal of Green Energy*, 13:4, 383-394, DOI: [10.1080/15435075.2014.961466](https://doi.org/10.1080/15435075.2014.961466)

To link to this article: <https://doi.org/10.1080/15435075.2014.961466>



Published online: 27 Oct 2014.



Submit your article to this journal [↗](#)



Article views: 308



View related articles [↗](#)



View Crossmark data [↗](#)



Citing articles: 2 View citing articles [↗](#)

Photovoltaic-thermal (PV/t) panel to minimize electrical and air conditioning energy consumption of a typical office in Beirut

S. Makarem, K. Ghali, N. Ghaddar, and S. Karaki

Department of Mechanical Engineering, Faculty of Engineering and Architecture, American University of Beirut, Beirut, Lebanon

ABSTRACT

A combined photovoltaic–thermal (PV/t) panel is proposed to produce simultaneously electricity and heat from one integrated unit. The unit utilizes effectively the solar energy through achieving higher PV electrical efficiency and using the thermal energy for heating applications. To predict the performance of the PV/t at a given environmental conditions, a transient mathematical model was developed. The model was integrated in a heating application for a typical office space in the city of Beirut to provide the office needs for electricity, heating during winter season, and dehumidification and evaporative cooling during the summer season. To minimize the yearly office energy (electrical and heat) needs, the PV/t panel cooling air flow rate and the dehumidification regeneration temperature were determined for optimal unit operation. Thermal energy savings of up to 85% in winter and 71% in summer were achieved compared to conventional systems at a payback period of 8 years for the panels.

KEYWORDS

Performance of photovoltaic–thermal panel; PV/t for heating dehumidification and power; sizing hybrid renewable system

Nomenclature

C	cost (\$)
C_f	thermal plant conversion factor
C_p	air specific heat, kJ/kg·°C
H	enthalpy, kJ/kg
h	heat transfer coefficient, W/m ² ·°C
I	energy, kWh
J	cost, \$
m	air mass flow rate, kg/s
P	power, W
PMV	predicted mean vote
PV/t	photovoltaic–thermal
RH	relative humidity
T	temperature, °C
X	absolute humidity, kg of H ₂ O/kg of dry air
Greek symbols	
ρ	density, kg/m ³
η	efficiency
Subscripts	
a	air
aux	auxiliary
c	combined
db	dry bulb
ec	evaporative cooler
el	electrical
f	fan
in	inlet
int	internal
out	outlet
pv	photovoltaic
pvt	photovoltaic/thermal
reg	regeneration
sky	sky
t	total
th	thermal
wb	wet bulb

Introduction

In the midst of the environmental problems, increasing fossil fuel prices, decreasing oil reserves and worldwide economic crises, mankind is continuously searching for an abundant source of energy that can efficiently replace fossil fuel. Renewable energy presents itself as the best solution, on top of which comes solar energy. Solar energy became widely used as a source of thermal energy (solar thermal collectors) mainly for the production of domestic hot water, and photovoltaic technology comes a close second.

Photovoltaic (PV) panels offer the advantage of transforming incoming solar radiation into electricity without any mechanical part, thus avoiding wear and tear in addition to costly maintenance. However, PV panels still face several limitations: they are not cost competitive because of their relatively high installation cost and their low electrical efficiencies. Photovoltaic panels' efficiencies are at best 19% (Parida, Iniyani, and Goic 2011), and in most cases in the vicinity of 10%, rarely reaching 15% for commercially available panels. Another serious problem is that PV cells' efficiency drops with increasing operating temperature: A drop of 15% in electrical efficiency can be seen for an increase of 30 degrees K in cell's temperature (Bergene and Lovik 1995). This disadvantage has led scientists to search for ways to counter the temperature effect on PV cells, and cooling the panels became an interesting topic for researchers. When the PV panel is cooled, and the extracted heat is used in any application, the panel is referred to as PV/thermal (PV/t). Photovoltaic thermal panels have a higher energy yield per unit area than separate systems of PV panels and solar collectors, which can be beneficial in densely populated areas. In addition, the electrical efficiency of the PV/t is higher than that of a standard PV panel

because of the reduced cell temperature (Kumar and Rosen 2011a,b). Photovoltaic thermal technology offers the advantage of providing both high-grade electrical energy and low-grade thermal energy. The increased electrical energy due to cell cooling, and the high thermal efficiency of the *PV/t* panel make the latter a more attractive alternative to conventional electricity, and make the panels more cost competitive since increased energy yield means a shorter payback period. *PV/t* applications are numerous and *PV/t* panels can be used in practically any application requiring low-grade thermal energy (Hu, Wang, and Fang 2010; Pei et al. 2013).

Cooling of PV panels can be done by air, water or water/glycol medium (Zondag et al. 2003). Cooling using water or water/glycol have higher thermal efficiencies due to higher heat transfer coefficients (Hedayatizadeh et al. 2013; Dubey and Tay 2014), but requires special design and manufacturing considerations, such as fluid tubes, thermal expansion of the fluid and possible fluid freezing during extreme weather. Air cooling on the other hand offers two main advantages: it can be installed on already existing systems with minimum complications, and the hot air being readily available for use in applications without the need for heat exchangers.

The air cooled panels are regular PV panels, provided with an air channel, and the various designs include: single air passage above or below the absorber, two air passages above and below the absorber in a single-pass or a double-pass. According to Hegazy (2000), numerical solutions of the energy balances show that the single air pass above the absorber has the lowest performance as compared to cooling the lower absorber side or the two sides of the absorber (above and below) in a single or double passes. However cooling the two sides of the absorber in a single pass requires the least fan power and provides comparable thermal and electrical output gains as the case of the double pass absorber air cooling. Cooling the panels by air was studied also by Garg and Adhikari (Garg and Adhikari 1999), who found that thermal and electrical outputs are directly proportional to collector length, air flow rate and packing factor, and inversely proportional to duct length. In another work, the combined effect of the air flow rate, the air channel depth, the length and the packing factor on the efficiency and outlet temperature was evaluated by Prakash (1994). The output temperature decreased with increasing the mass flow rate, while the thermal efficiency increased. To improve the performance of air cooled *PV/t* panels, the addition of fins was considered in several papers. For example, Kumar and Rosen (2011a,b) evaluated the performance of a double-pass *PV/t* solar air heater with and without fins. They found out that the addition of fins in their model increased the thermal and electrical efficiencies to 15.5% and 10.5%. Other studies conducted by Tonoui and Tripanagnostopoulos (2007a,b) showed that adding a suspended plate to enhance heat transfer to the air, increased the energy efficiency from 25% to 28%, while adding fins allowed the energy efficiency to reach 30%. The study also suggests that the use of fins is more beneficial where higher heat gains are required in winter, while a suspended plate design is preferred for tropical countries.

Air cooled *PV/t* panels are usually used to offset the heating load of houses during winter, and successfully implemented

systems are widely used in cold countries like Canada. Thermal energy extracted from *PV/t* panels is also being used to provide summer cooling: it is either used in absorption cycles, or in desiccant systems [Hammoud, Ghali, and Ghaddar 2014; El Hourani, Ghali, and Ghaddar 2014]. For example, the feasibility of flat plate *PV/t* modules was studied by Vokas, Christandonis, and Skittides (2006), where the thermal energy is used for space heating and cooling. The *PV/t* thermal efficiency was found to be 9% lower than the efficiency of a conventional solar collector. Mei et al. (2003) designed and tested a *PV/t* air collector system to meet the heat requirements of a desiccant cooling machine (DCM), to satisfy part of the cooling load of Mataro Library, near Barcelona. Several additional solar collectors were needed to achieve the desired air temperature of 70°C, which was found to be sufficient to regenerate the DCM, thus reaching a solar fraction of 75%. The use of *PV/t* collectors with desiccant cooling systems was also studied by Beccali, Finocchiaro, and Nocke (2009). In their study, the DCM was connected to a single glazed standard collector and a *PV/t* air collector.

It is clear that intensive research has been conducted on enhancing the electrical and thermal performance of *PV/t* panels and on the use of the extracted heat in different applications for heating and cooling. However, the use of the *PV/t* panels in the city of Beirut has not been investigated despite the abundance of solar energy which can be harnessed not only for producing photovoltaic electricity but also for extracting thermal energy for winter heating and summer desiccant cooling. In this study, the *PV/t* panels will be considered to minimize the seasonal energy cost (electrical and thermal) of an office in the city of Beirut. The work will focus on optimizing the required airflow that will enhance electrical output of the *PV/t* panels and minimize the thermal heating needs for regenerating the desiccant wheel during the summer cooling season. Whereas in winter, the optimized airflow will minimize both the office electric energy dependence and the space heating needs. The objectives can be summarized as follows: (1) Develop a simulation model that can predict the performance of the *PV/t* panels at different ambient conditions and cooling air flow rates. (2) Integrate the *PV/t* model with a space model, a desiccant model and an evaporative cooler model to predict the energy performance of the combined system and (3) Optimize the system's operation for lowest operating cost while maintaining thermal comfort.

System description

The *PV/t* panels are integrated in a heating and cooling system for a typical office space in Beirut (see Figures 1 and 2). The extracted heat is used to reduce the auxiliary heat requirement for winter heating, as well as to reduce the auxiliary heat needed to regenerate a desiccant cooling system in summer. The proposed desiccant cooling system uses the desiccant (Silica gel) to decrease the humidity of the fresh air stream passing through the desiccant wheel. The system thus eliminates the need for the conventional and energy extensive dehumidification that relies on lowering the air temperature below the dew point and then reheating to the supply temperature. The desiccant is then regenerated by hot air: the hot air

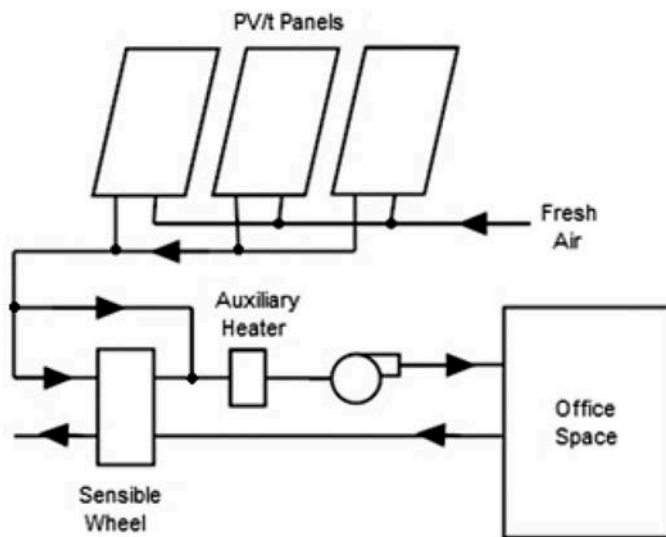


Figure 1. System operation during Heating Season.

stream removes the absorbed water from the desiccant allowing it to regain its dehumidification characteristic. The result of using the desiccant system is a dry air stream capable of removing the space's latent load. In order to remove the sensible load as well, the air must enter the space at a relatively low temperature: lowering the air temperature is accomplished by using an evaporative cooler.

The air required for the regeneration process is heated before entering the desiccant wheel. This heating is normally done by conventional means, i.e. fuel or gas. In this study, the air enters the *PV/t* panels prior to the auxiliary heater: this has the double advantage of not only reducing the required amount of gas for the heater, but also of reducing the *PV/t* panels' operating temperature which will increase their electrical efficiency. For this to take place efficiently, the air entering the panels needs to have a temperature low enough to cool them; thus the configuration of Figure 1 is chosen for the heating season and the configuration of Figure 2 for the cooling season. The hot air supplied by the *PV/t* panels (placed in a parallel formation) is used to regenerate the desiccant wheel to dehumidify the office supply air. The dehumidified air is then cooled by the office exhaust air, heat sink, and finally by an evaporative cooler before being injected into the space. During the heating season, the outside fresh air is heated in the panels, then passes in a sensible

wheel for heat recovery from extracted air; if, at the outlet of the sensible wheel, the process air is not hot enough to meet the heating load inside the space, it will be further heated in an auxiliary heater. If the air exiting the panels is capable to meet the heating load without further heating, it bypasses the sensible wheel and is injected directly into the space, as shown in Figure 1.

The air flow rate circulated in the system is dependent on the cooling load (or heating load) that requires to be met in order to maintain thermal comfort in the office: this constraint ties the office thermal comfort requirements to the electric output of the *PV/t* panels. Increasing the office air flow rate will increase the panel electrical and thermal efficiencies at the expense of an increase in the fan power consumption, and an increase in the thermal energy needed to maintain the air at the required regeneration temperature.

Mathematical modeling

In order to predict the system's performance, mathematical models for different system components are needed. A *PV/t* model is developed to predict its performance at different ambient conditions. The *PV/t* model is integrated with desiccant and thermal space models to optimize the operation of the integrated system (*PV/t*, desiccant and evaporative cooler) to provide the office space needs for thermal comfort, air quality and electricity at a minimal energy cost.

Photovoltaic-thermal model

The *PV/t* panel under study has two air passages above and below the absorber with double pass configuration, as shown in Figure 3. The channel depths are chosen to be 3 cm for the upper channel and 3 cm for the lower channel since this configuration, combined with these channel depths, yields the highest thermal and electrical efficiencies with acceptable pressure drop (Kumar and Rosen 2011a,b). The determination of the *PV/t* performance is predicted by performing one dimensional steady state heat transfer analysis based on the mathematical formulation of Kumar and Rosen (2011a,b); Kumar considered the superstrate as an additional layer and included the heat conducted from the superstrate to the absorber in the calculation to improve the model's accuracy. This model takes as inputs the outdoor temperature, the air mass flow rate, the solar irradiance on the *PV/t* surface, the

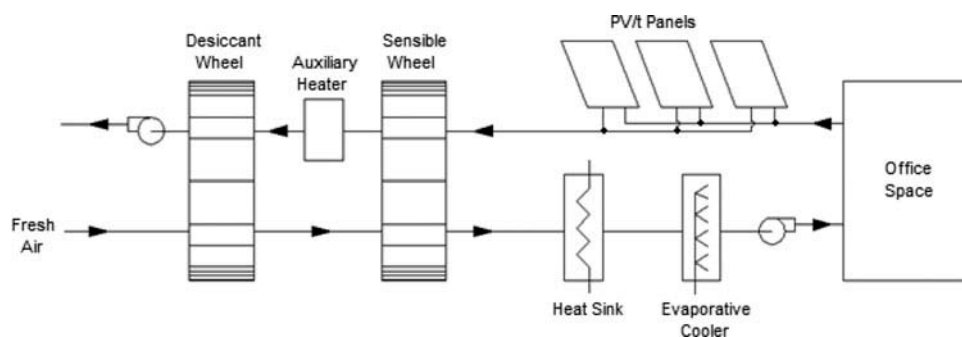


Figure 2. System operation during Cooling Season.

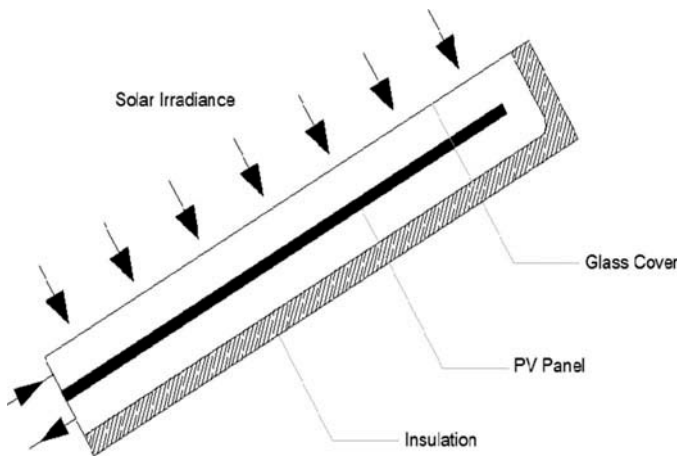


Figure 3. Schematic of the PV/t panel.

inlet air temperature, the wind speed and the cells' packing factor (taken here equal to 0.9), and calculates the air temperature at the outlet of the PV/t, as well as the mean cell temperature, which are used to calculate the thermal and electrical efficiencies, respectively. This model was validated by Kumar and Rosen (2011a,b).

Desiccant model

The desiccant machine consists of a rotary wheel, divided into two sections, for two counter-flow air passages. In one passage, the hot dry air regenerates the desiccant and is then exhausted to the outside, and in the other passage the air is dehumidified before being cooled by the evaporative cooler, and then supplied to the office building.

This study uses the model presented by Beccali, Adhikari, and Butera (2004) to predict the properties of the air exiting the desiccant wheel. This model presents empirical correlations for the temperature and humidity ratio of the air exiting the adsorption compartment of the desiccant wheel as a function of the properties of the regeneration air and the outdoor air based on wide-ranging experimental data for different types of desiccant materials. The model of Beccali allows for the direct calculation of the enthalpy and relative humidity of the air exiting the desiccant wheel by the following correlations:

$$H_{out} = (0.1312H_{reg} + 0.8688H_{in}) \quad (1)$$

$$RH_{out} = (0.9428RH_{reg} + 0.0572RH_{in}) \quad (2)$$

where H_{out} , H_{reg} , and H_{in} are, respectively, the enthalpy of the air exiting the desiccant wheel, the regeneration air and the air entering the adsorption compartment while RH_{out} , RH_{reg} , and RH_{in} are, respectively, the relative humidity of the air exiting the desiccant wheel, the regeneration air and the air entering the adsorption compartment. Beccali presented the correlation shown in Eq. (3) allowing for the calculation of the air temperature T_{out} exiting the desiccant wheel by:

$$\frac{RH_{out}e^{0.053T_{out}} - 1.7976}{18671} = \frac{h_{out} - 1.006T_{out}}{2501 - 1.805T_{out}} \quad (3)$$

This model has been used by many researchers due to its simplicity and its wide range of applicability. The model correlations are valid for inlet temperatures between 20°C and 34°C, regeneration temperatures between 40°C and 80°C, inlet air humidity ratio between 8 and 15 g/kg, and regeneration air humidity ratio between 10 and 16 g/kg.

Evaporative cooler model

The evaporative cooler model presented by Kinney (2004) is used. The performance factor (PF) was assumed to be equal to 90%, which is a property of a good quality evaporative cooler as found by Kulkarni and Rajput (2011) who studied the performance of several commercially available evaporative coolers including paper, rigid cellulose, polythene and aspen fiber. The air outlet temperature is calculated using Eq. (4).

$$T_{out,EC} = T_{db,in} - PF \times (T_{db,in} - T_{wb,in}) \quad (4)$$

Space model

A space model is needed to calculate the transient heat transfer through the multi-layered walls to predict the indoor conditions and the resulting thermal comfort. The space model used in this paper was already used in the work of Yassine et al. (2012) and validated using TRNSYS (2010) software. The transient one-dimensional heat conduction equation for the office's envelope components consisting of N parallel layers is given by:

$$\rho_{i,j}c_{i,j} \frac{\partial T_{i,j}(x,t)}{\partial t} = k_{i,j} \frac{\partial^2 T_{i,j}(x,t)}{\partial x^2} \quad (5)$$

where i is the building element type, j is the layer number, k is the element's thermal conductivity, ρ is the element's density, and c is the element's specific heat. The wall outside surface boundary conditions is expressed by:

$$\begin{aligned} \alpha I(t) + h_{c\infty}[T_{\infty}(t) - T_i(0,t)] + h_{r\infty}[T_{sky}(t) - T_i(0,t)] \\ = -k \frac{\partial T_{i,j}(0,t)}{\partial x} \end{aligned} \quad (6)$$

where $h_{r\infty}$ is the external radiative heat transfer coefficient, I is the total solar radiation, $h_{c\infty}$ is the external convective heat transfer coefficient, T_{∞} is the outdoor temperature and T_{sky} is the sky temperature.

The wall inside surface boundary conditions can be expressed by:

$$\begin{aligned} h_{ca}[T_i(L,t) - T_a(t)] + \sum_{j=1}^6 h_{ri-j}[T_i(L,t) - T_j(t)] \\ = -k \frac{\partial T_i(L,t)}{\partial x} \end{aligned} \quad (7)$$

where $h_{r,i-j}$ is the internal radiative heat transfer coefficient, h_{ca} the convective heat transfer coefficient of room air, and T_a the room air temperature. The expression for the internal lumped air energy balance is given by

$$\rho_a V_a c_{pa} \frac{\partial T_a(t)}{\partial t} = \sum_{i=1}^6 h_{c,a} A_i (T_i - T_a) + \dot{m}_a c_{pa} (T_{supply} - T_a) + \sum q_{int} \quad (8)$$

where q_{int} is the internal heat gain and V_a is the room air volume. The moisture balance in the space is expressed by:

$$\rho_a V_a \frac{\partial W_a}{\partial t} = G - \dot{m}_a (W_a - W_{supply}) \quad (9)$$

where G is the moisture generation rate in the room, W_a and W_{supply} are the room air humidity ratio and the supply air humidity ratio, respectively.

The PMV is then calculated using the predicted indoor air temperature and humidity (Fanger 1982); the PMV should have a value between -0.5 and 0.5 to indicate thermal comfort (this corresponds to less than 10% of people dissatisfied).

Objective function

The integrated system variables are the total air mass flow rate and the regeneration temperature. When these variables change in the system, the outputs can change noticeably. For example, increasing the mass flow rate of the air cooling the panels will not only increase both thermal and electrical efficiency, but also increase the fans electrical consumption and decrease the outlet temperature of the air which affects the desiccant regeneration, since we need a minimum temperature of 50°C for effective regeneration. The decrease in PV/t air outlet temperature increases the needed auxiliary energy to maintain the air stream at the required regeneration temperature, thus increasing the operating cost. The best operating conditions which reflect the minimum operating cost cannot be found in a straight forward manner; this is why optimization is needed.

The objective is to minimize the cost of energy needed to run the cooling/heating system in the office space while maintaining thermal comfort. The cost function to be minimized is presented by:

$$J = C_g \times I_{elec} + C_{aux} \times (I_{th} - I_{PVt}) + C \times (e^{PMV^2} - 1) \quad (10)$$

$$I_{elec} = I_t - I_{PV} = I_{office} + I_f - I_{PV} \quad (11)$$

where

- I_{elec} is electrical energy bought from the grid [kWh];
- I_t is the total energy consumed by the office's equipment and the system [kWh];
- I_{th} is the total thermal energy needed for regenerating the desiccant [kWh];
- I_{PVt} is the thermal energy provided by the PV/T panels [kWh];

- I_{PV} is the excess electrical energy provided by the PV [kWh];
- I_{office} is the electrical energy consumed by office appliances [kWh];
- I_f the electrical energy consumed by the fans [kWh];
- PMV is the predicted mean vote [unitless].
- C_g , C_{aux} , and C are the cost of buying and selling electricity [\$/kWh], cost of gas [\$/kWh], and the weighing factor for thermal comfort [\$], respectively.

The power required to run the fans is calculated using Eq. (12), where \dot{m} is the air mass flow rate [kg/s], ΔP is the pressure drop across the system [Pa] ($\Delta P = 900$ Pa), and η_{fan} is the fan efficiency, taken as 80%.

$$P_f = \dot{m} \times \frac{\Delta P}{\eta_{fan}} \quad (12)$$

Numerical simulation

The system operates during hours of occupancy from 7 a.m. till 5 p.m., and only ventilation is on during the night. The simulation of the integrated models starts by finding the room conditions when the system is still off; this is done by running the space model alone for the whole night in order to reach steady state conditions during the first hour of occupancy which will serve as a starting point for the system. The physical properties of the space (wall construction), occupancy and equipment, and weather data are input to the system. The walls are discretized into 120 nodes, and a time step of 20 seconds is used to perform the iterations for each hour of study until steady state is achieved. The mass flow rate and regeneration temperature are the decision variables, and their optimum values corresponding to the lowest cost are found using the optimizer. The optimizer of choice is the genetic algorithm with the following parameters: population size is set to 20, crossover fraction set to 0.2, the elite count is set to 2, 100 generations are accounted for and the tolerance function is set to 1×10^{-6} . The genetic algorithm starts by randomly seeding the first generation of decision variables. The cost is calculated for each combination of these variables, and only the fittest variables (i.e. those resulting in minimal cost) are used in the next generation. This procedure is repeated until the difference in the cost is less than the pre-set tolerance function.

In this study, the decision variables are the air mass flow rate and the regeneration temperature, and as shown in the chart (Figure 4) the optimizer proceeds by randomly seeding their values to form the first generation. The space model discretizes the different room elements (walls, ceiling, ...) and uses the explicit method to calculate on an hourly basis the heat transferred into the space from the outside, and the generated heat from the equipments and occupants. The PV/t model calculates the generated electricity and the air outlet temperature at the corresponding air flow rate. The conditions of the fresh air intake (now referred to as process air) exiting the desiccant wheel are found using the desiccant model. The process air temperature is calculated at the outlet of each of the sensible wheel and the heat sink, and the supply temperature and

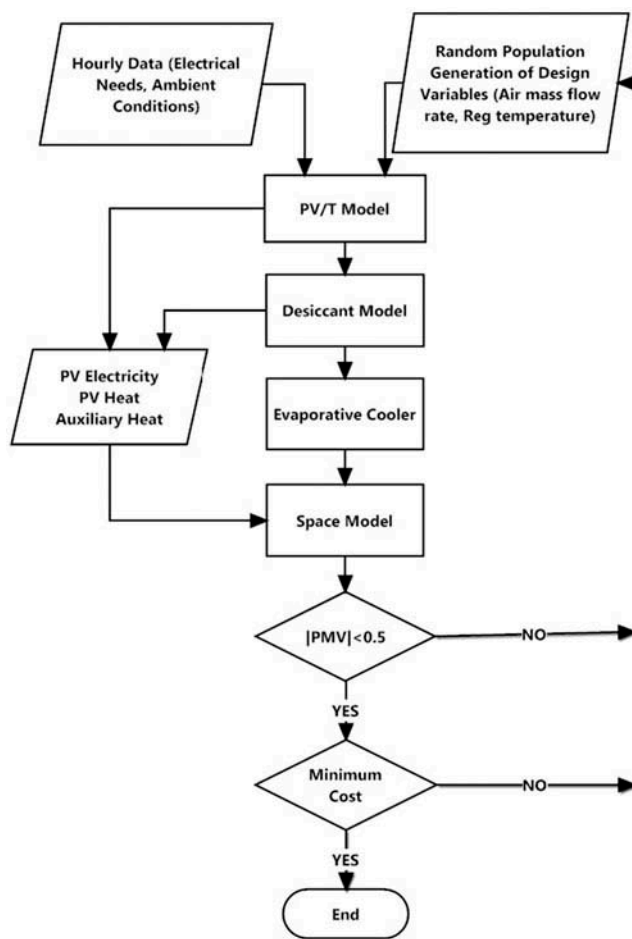


Figure 4. Flow chart of the optimization methodology.

humidity are calculated using the evaporative cooler model. The supply conditions are then fed to the space model to calculate the room temperature, room humidity and *PMV*. The optimizer then interprets the results: if the minimum operating cost was found and thermal comfort is achieved, the optimizer moves to the next hour for analysis. If not, a new set of decision variables—based on the most fit variables of the previous generation—is generated and the simulation is repeated. Once the optimum values of the flow rate and regeneration temperature are found for an hour, the optimizer uses the current room conditions as a starting point for the next hour's optimization. The simulations are done for the occupancy hours between 7 a.m. and 5 p.m.

Case study

The system is applied on a typical office space in Beirut, and the electricity needed for internal use (computers and lighting) is to be supplied by a *PV* system, with no electricity storage (on-grid system); for this purpose the *PV* system will be sized as to generate electric energy throughout the year equal to the yearly electric consumption of the office. The on-grid system means that electricity will be bought from the grid during shortage, and the excess electricity will be sold. Both

the heating and cooling systems of the office have heat as a common source of energy, and this heat is obtained from gas combustion. The *PV* system is sized to meet the yearly electric consumption using HOMER¹ software. As a mean to cool the panels and to have higher electrical efficiency, heat will be extracted from the panels to meet part of the thermal needs of the system. The objective is to check the system's feasibility, and to optimize the system's performance in order to provide adequate cooling for the *PV* panels and generate more electricity, extract the thermal energy from the *PV/t* panels to minimize the need for the auxiliary heat (gas), i.e. minimize the system's operation cost, all while maintaining thermal comfort inside the space. Once the optimization is complete, the savings on electricity and gas will be investigated as well as the payback period for installing the *PV/t* panels.

The office is an 8 m × 8 m × 3 m space in Beirut with a constant occupancy of 5 people from 7 a.m. til 5 p.m. The room has two outside walls facing South and West, the Eastern and Northern walls are partition walls and the floor (ceiling) is above (below) conditioned space; the construction characteristics are shown in Table 1. The weather data used (solar irradiance, outdoor temperatures and humidity) are taken from the weather station in the American University of Beirut. The office in this study includes 5 desktop computers each requiring 150 W, and the lighting load is assumed to be 11 W/m². The total electrical load of the office is 1.45 kW/working day. A DC/AC converter will be needed, its efficiency is assumed at 95%, and additional losses equal to 10% are considered; these efficiencies are used for calculating the electrical power needed to be provided by the panels which would be 1,700 W. The system is an on-grid *PV/t* assisted desiccant system that will provide cooling and heating to the office space during the hours of operation, and reduce the electricity bill by generating electricity from the *PV/t* panels and selling the excess electricity to the grid.

During cold season, heating is accomplished by burning gas. The optimized system will provide part of the needed heat from the extracted thermal energy from the *PV/t* panels. January is considered as a representative month for the heating season; in this case, the air mass flow rate in the system has the range between 0.1 kg/s and 2 kg/s; the range was chosen to account for the minimal ventilation rate. If the air temperature of the air at the inlet of the heater is enough to heat the space, the auxiliary heater is considered off by the system. Since the mass flow rate has the main influence on the system's behavior during heating operation, it is the only variable, and the hourly flow rate resulting in the minimum operation cost is found.

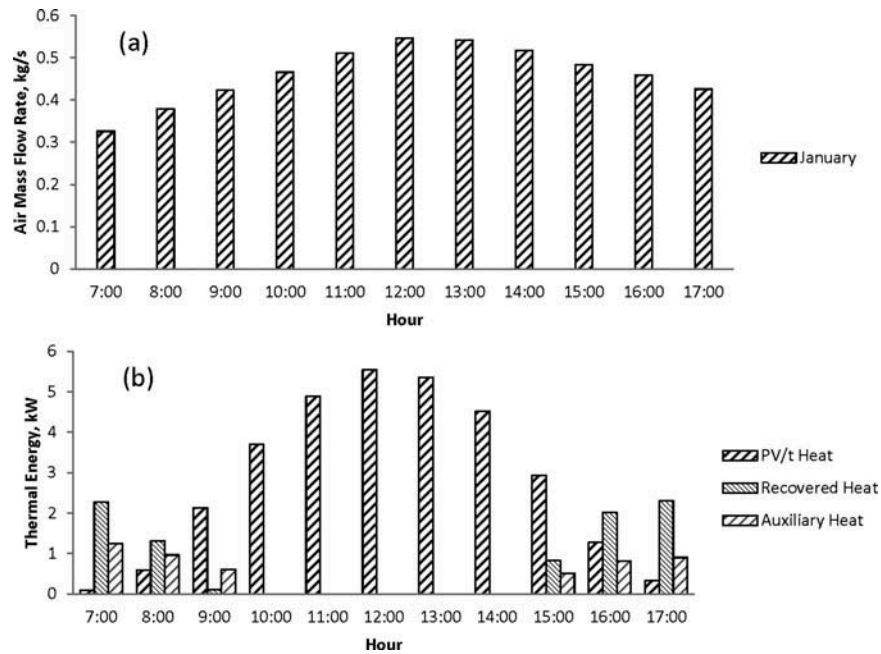
During cooling season, the cooling is accomplished by a desiccant cooling system: the desiccant dehumidified the air which is cooled later on by evaporative cooling. April represents a typical spring weather, and August and September represent summer weather. A representative day (21st) will be studied for each of these months. During these months, the air mass flow rate and regeneration temperature ranges are 0.1–2 kg/s and 50–80°C, respectively.

At any time, the excess electricity is sold to the grid at the same price it is bought, for this reason the objective would be to generate an amount of electricity equal to that consumed

¹Laboratory National Renewable Energy. HOMER Software. Colorado, USA

Table 1. Wall construction characteristics.

Wall Layer	Thickness mm	Density kg/m ³	Specific Heat kJ/kg-K	Thermal Conductivity W/m-K
Plaster	15	1860	1.09	0.72
Concrete Hollow Block	200	608.7	0.84	0.38
Plaster	15	1860	1.09	0.72

**Figure 5.** Schematic of a) hourly mass flow rates; b) hourly thermal energies in January.

throughout the year. Based on manufacturer data, the PV panel has a peak power of 200 W output under Standard Test Conditions (1000 W/m²), 25°C and a surface area of 1.6 m². The PV/t panels are placed facing South with a constant inclination angle of 30° to avoid seasonal adjustments; this tilt angle is considered since the location's latitude is 33°54N. For the PV system sizing HOMER² software is used. HOMER takes as inputs the location's latitude and longitude, the panel orientation and tilt angle, the panel's efficiency at the normal operating cell temperature (NOCT), the total daily solar radiation on a horizontal surface and the mean monthly outdoor temperature. Several cases (PV systems sizes) are then entered so HOMER can find the best applicable option; HOMER then takes into account the effect of the cell temperature on the efficiency, the inclination angle and orientation, calculates the electricity production, and determines the optimum PV system size. The best system size found by HOMER for this case study has a capacity of 4 kW, or 20 PV panels (200 Wp, 12.5% electrical efficiency at NOCT) and is found to meet the previously mentioned criteria: total yearly electricity production equal to total yearly consumption.

Taking into account the needed space between the panels, the required space to install them is 3.8 m × 10 m, equivalent to 60% of the roof area, leaving enough space for other mechanical equipments.

The cost of buying and selling electricity found in the objective function (Eq. (10)) is $C_g = 0.09\$/\text{kWh}$, the cost of

buying gas is $C_{aux} = 0.05\$/\text{kWh}$; these prices are the average prices in the Lebanese market. The weighing factor ($C = 8$) is chosen to give an equal weight (importance) between the thermal comfort criteria and the cost of energy.

Results and discussion

The system is first set to heating (see Figure 1) and January is chosen as a representative month for winter. In this case the variable is the mass flow rate and its hourly values are found to minimize the system's operation cost while maintaining thermal comfort. The total mass flow rate and the auxiliary heat to be supplied to the system are shown in Figure 5(a and b) respectively. As can be seen in Figure 5(a), the air flow rate increases throughout the day then decreases, following the trend of the solar radiation: as the solar radiation on the panels increases, the PV cells' temperature increases, so does the air temperature at the panels' outlet. This requires a higher flow rate to cool the panels on one hand, and to reduce the supply temperature on the other hand to avoid overheating the space.

During early morning and late afternoon, a certain amount of auxiliary heat is required to meet the heating load. The low flow rates at these hours are due to the low solar irradiance, thus the reduced amount of air needed to cool the panels. As the solar irradiance and the outside air temperature increase, the thermal energy absorbed from the panels increases. The

²Laboratory National Renewable Energy. HOMER Software. Colorado, USA

auxiliary energy is only used to offset the deficit in solar thermal energy in meeting the space heating load. When the temperature of the air at the outlet of the *PV/t* panels is higher than the return temperature, the air stream bypasses the sensible wheel (see Figure 1). The absence of added auxiliary heat between 10 a.m. and 2 p.m. indicates that the panels are sufficient to meet the heating load during these hours. Table 2 shows the supply temperatures and the space temperatures at different hours. The supply temperature is seen to change between 23.3°C in the morning due to low outdoor temperature, and 22°C in the afternoon where there is a slight increase in outdoor temperature.

To simulate the performance of the system in cooling mode, the optimizer was run during April, August, and September. The monthly load profile is shown in Figure 6, where it is clear that the load removed by the system increases throughout the day, and decreases in the late afternoon. The horizontal line represents the internal load (occupants, equipments and lighting). It can be noticed that at 7 a.m. in April, the load removed by the system (showed in bars) is smaller than the internal load: the difference between the two loads is actually the load removed by the office walls since during these hours, the outdoor temperature is lower than the room temperature, and heat is conducted out of the space through the walls. The space peak loads are found in Figure 6 at 3 p.m., and the peak loads per square meter for April, August and September are 40.9 W/m², 42.8 W/m², and 43.4 W/m², respectively.

The resulting mass flow rates and regeneration temperatures are presented in Figure 7(a and b). It is observed that the higher the space cooling load, the higher the flow rate and the regeneration temperature. August and September are characterized by higher cooling loads than April, and this is reflected

in their higher mass flow rates and regeneration temperatures. At 7 a.m. the load is minimum, and the regeneration temperature for the three months is at its minimum of 50°C. As the cooling load increases, the system responds by increasing the flow rate, thus increasing its heat removal capacity; this is accompanied by an increase in the regeneration temperature, resulting in dryer air at the inlet of the evaporative cooler which increases its cooling capacity. At 1 p.m., the mass flow rate has increased to reach its peak of 0.48 kg/s (0.024 kg/s/panel), 0.55 kg/s (0.027 kg/s/panel) and 0.52 kg/s (0.026 kg/s/panel) for April, August and September respectively. The regeneration temperature increased as well and reached 63°C, 66°C and 65°C, respectively.

The calculated supply and room temperatures and the resulting PMV are shown in Table 3 for April, August and September. The system found the flow rates and regeneration temperatures corresponding to the lowest operating cost while maintaining thermal comfort, i.e. the operation at a *PMV* = 0.5 or slightly less. And since the internal load in the office is taken to be constant, the supply conditions are quasi steady; the variation in the mass flow rate and regeneration temperature reflects mainly the variation in the outdoor conditions (external load).

Figure 8 shows the hourly *PV/t* power generation for the different months. January has the lowest power generation because of low solar radiation reaching the panels, and between 10 a.m. and 1 p.m. the power generation exceeds the production, however over the whole day the generation is still less than the consumption. As the solar irradiance reaching the panels increases from April to August, so does the power generation, and the excess is now enough to cover for the electricity deficit during low irradiance hours. The monthly electricity production for the panels **before (after)**

Table 2. Supply and space temperatures.

		Hour of the Day									
		7-8	8-9	9-10	10-11	11-12	12-13	13-14	14-15	15-16	16-17
Jan	T_{supply} (°C)	23.35	22.9	22.7	22.4	22.3	22.1	22.05	22	22	22
	T_{space} (°C)	21.28	21.3	21.33	21.37	21.4	21.43	21.42	21.39	21.37	21.32

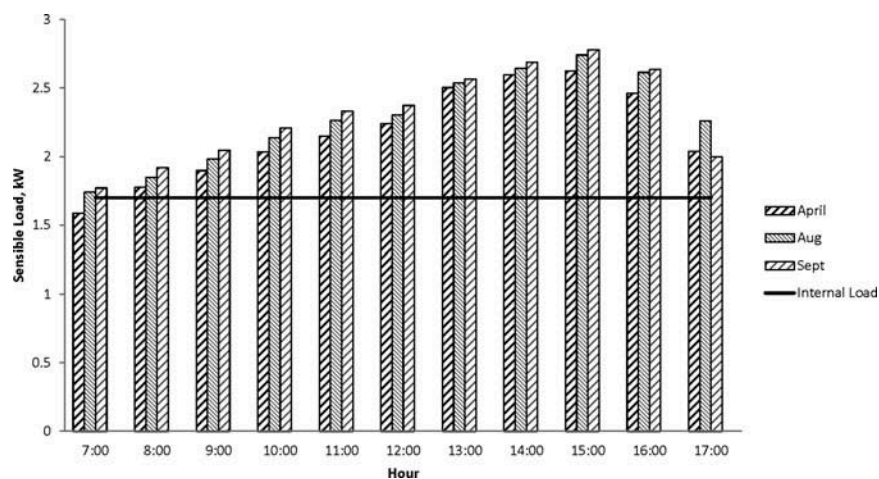


Figure 6. Hourly office cooling load.

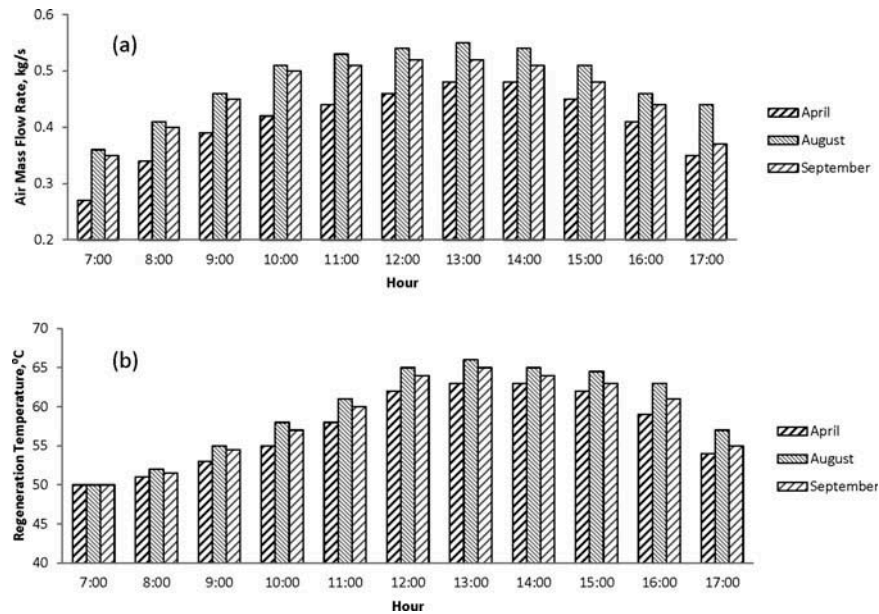


Figure 7. Schematic of a) hourly mass flow rate; b) hourly regeneration temperature in cooling season.

Table 3. Supply and space temperatures and PMV.

		Hour of the Day									
		7-8	8-9	9-10	10-11	11-12	12-13	13-14	14-15	15-16	16-17
Apr.	T_{supply} (°C)	18.7	19.1	19.38	19.4	19.23	19.23	18.95	18.73	18.35	18.27
	T_{space} (°C)	23.68	23.64	23.65	23.67	23.61	23.61	23.66	23.65	23.65	23.67
	PMV	0.5	0.49	0.49	0.5	0.49	0.5	0.49	0.5	0.5	0.5
Aug.	T_{supply} (°C)	19.55	19.8	19.95	19.98	19.81	19.81	19.43	19.1	18.8	18.56
	T_{space} (°C)	23.7	23.7	23.71	23.69	23.64	23.62	23.59	23.69	23.69	23.69
	PMV	0.5	0.5	0.5	0.5	0.49	0.49	0.48	0.5	0.5	0.5
Sept.	T_{supply} (°C)	19.15	19.5	19.67	19.69	19.52	19.52	19.15	18.92	18.41	18.25
	T_{space} (°C)	23.59	23.68	23.68	23.64	23.64	23.64	23.63	23.7	23.68	23.68
	PMV	0.48	0.5	0.5	0.49	0.49	0.5	0.5	0.5	0.49	0.49

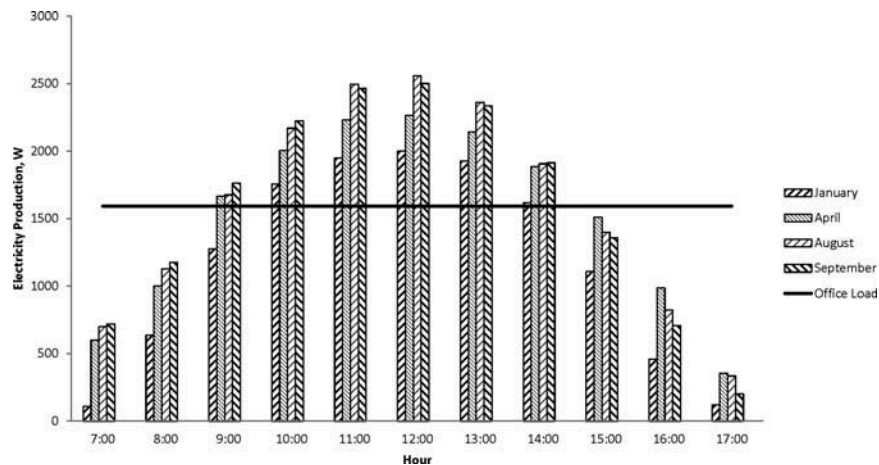


Figure 8. Plot of the hourly PV/t power generation.

optimization for January, April, August and September is 333 kWh (337 kWh), 410 kWh (428 kWh), 447 kWh (474 kWh) and 420kWh (440 kWh), respectively; The yearly electricity generation before optimization given by HOMER is equal to 5.2 MWh; the yearly consumption being equal to 5.18 MWh, the panels provide, before optimization, an electrical energy equal to that consumed. After optimization, 5.4 MWh are

generated throughout the year, making an improvement in electrical energy output of 4% due to the air cooling of the panels.

The thermal energy extracted from the PV/t panels is shown in Figure 9. The thermal energy follows the trend of the solar radiation on the panels, however it is also enhanced by the increase in the air mass flow rate during the day.

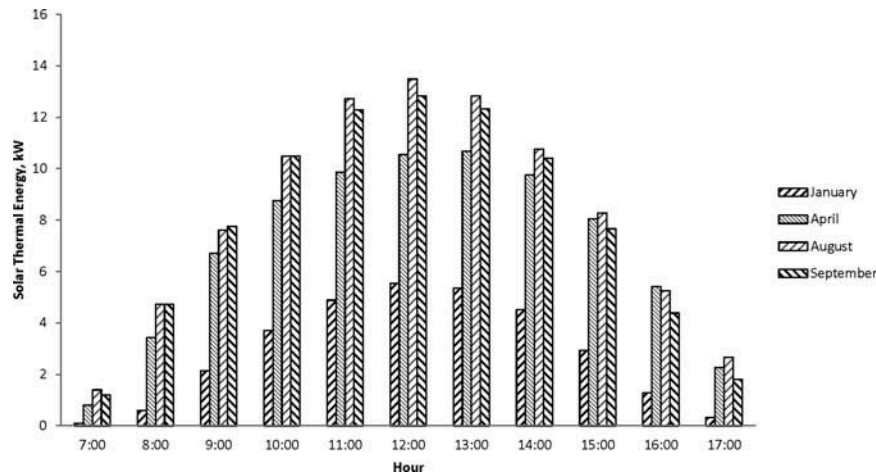


Figure 9. Plot of the hourly solar thermal energy.

August is characterized by the highest total extracted thermal energy followed by September and April. January is shown to have significantly less heat extracted, however the savings in thermal energy in January reach 85%, while savings in cooling season are around 71%: this is due to the higher thermal requirement for desiccant dehumidification (see Table 5).

Table 4 shows the electrical, thermal and combined efficiencies for the different months. The combined efficiency is calculated using Eq. (13).

$$\eta_c = \eta_{th} + \eta_{el}/C_f \quad (13)$$

$$\eta_{el} = \frac{P_{el}}{Irr \times A} \quad (14)$$

$$\eta_{th} = \frac{\dot{m} \times c_{pa} \times \Delta T}{Irr \times A} \quad (15)$$

where C_f is the conversion factor of the thermal power plant, and is taken equal to 0.38 (Kumar and Rosen 2011a,b), P_{el} is the electric power generated by a single PV/t panel [W], \dot{m} is the air flow rate in each panel [kg/s], c_{pa} is the air heat capacity [kJ/kg.K], ΔT is the rise in air temperature exiting the panel, Irr is the solar irradiance on the panel [W/m^2], and A is the panel surface area [m^2].

It can be noticed from Table 4 that the electrical efficiency in January is higher than in other months, this is mainly due to the lower operating cell temperature. During spring and summer, the increase in cell temperature results in a drop in the electrical output, leading to higher electrical efficiencies in the morning and afternoon, and the lowest efficiencies coinciding with higher irradiance. The air mass flow rate cannot be increased beyond its current values to obtain further cooling for two reasons: first, the optimization is done for the whole system operation, and not only for the PV/t panels, and second, the current flow rates, coupled with the regeneration temperatures, ensure the system operation at minimum cost: increasing the flow rate would certainly increase the electrical and thermal efficiencies, and the electrical output of the PV/t panels, however it will also increase the operation cost.

On the other hand, the thermal efficiency, defined as the ratio of the heat extracted to the total radiation on the panels (see Eq. (15)), is affected by the solar irradiance, the mass flow rate in the panels and the ambient temperature. The thermal efficiency is found lowest in the morning since the ambient temperature, the irradiance and the mass flow rate are all at their lowest values. The thermal efficiency increases throughout the day with the increase of the solar radiation, and in the afternoon when the solar radiation starts to decrease, the thermal efficiency keeps increasing in April, August and September, whereas it decreases in January: this is explained by the low heat loss from the panels to the environment in the

Table 4. Electrical and thermal efficiencies (%) of the PV/t panels.

		Hour									
		7-8	8-9	9-10	10-11	11-12	12-13	13-14	14-15	15-16	16-17
Jan.	η_{el}	12.4	12.4	12.2	12	11.7	11.7	11.9	12	12.1	12.1
	η_{th}	29	41.9	45.7	47	48.2	47.8	47.4	42.7	34	28
	$\eta_{combined}$	62.4	74.5	77.8	78.6	79	78.6	78.7	74.3	65.8	59.8
Apr.	η_{el}	10.2	9.6	9.3	9.27	9.23	9.3	9.5	9.8	10.2	10.8
	η_{th}	30	35	37.8	39.7	41.2	43	44.5	45.7	46.2	49
	$\eta_{combined}$	56.8	60	62.4	64	65.5	67	69	71	73	77
Aug.	η_{el}	10.1	9.7	9.3	9.15	9.12	9.2	9.6	10	10.4	10.8
	η_{th}	35.7	38	40	42.3	43.6	45	46.8	49.7	53	60
	$\eta_{combined}$	62.4	63.6	64.7	66	67.6	69.3	72	75.6	80.7	88
Sept.	η_{el}	10.1	9.6	9.2	9	9	9.2	9.57	10	10.6	11
	η_{th}	35.5	39.3	42	43	44.7	45.5	46.8	48.8	52	58
	$\eta_{combined}$	62.3	64.5	66	67.5	68.5	69.7	72	75.2	80	87

Table 5. Electric and thermal energy consumption.

	January	April	August	September
Electricity Consumption, kWh	395.3	395.3	395.3	395.3
PV Generation, kWh	337	428.3	473.5	439.6
Heat Requirement, kWh	801.8	3236.6	4028.6	3745
PV/t Thermal Heat, kWh	681.1	2413	2884	2685

cooling season, in contrast to higher heat loss in January due to the more significant outdoor temperature drop in the afternoon during that month. The combined efficiency follows the trend of the thermal efficiency, and the average overall efficiencies of April, August and September are 66.5%, 71%, and 71.2%, respectively.

Table 5 presents the monthly electric and thermal energy consumption and generation for the months of study; the calculations were done based on a representative day (21st), then multiplied by each month's number of days. In January, due to low solar irradiance reaching the panels, the electricity generation is less than the consumption, which is predictable. The thermal production is enough to achieve savings up to 85%. During the months of higher solar irradiance, the electricity generation is found higher, with savings exceeding 100%, i.e. the electricity production exceeds the consumption. August has the highest electricity production (highest solar irradiance and highest electrical efficiency), followed by September and April.

The system was compared to a conventional desiccant cooling system, and the savings in the new system on auxiliary and electric energy were calculated, and these savings are used to calculate the payback period of the installed PV/t panels. We assumed we have three months of heating, six months of cooling, and 3 months with no need for neither heating nor cooling. January being the representative month for the heating season, the thermal energy consumption in each of the heating months (December through February) is equal to that in January. The cooling season considered from April till September is represented by the three months studied: April, August and September; and the savings in thermal energy in May, June and July are considered equal to those of April, September and August, respectively. The price of the PV/t panels is assumed to be 10,500\$ including the installation and the accessories.

The price of electricity is taken equal to the cost of electricity production in Lebanon, which is equal to 0.17\$/kWh (Ruble and Karaki 2013), and a yearly interest rate of 4% is assumed. When the Photo-voltaic panels are considered alone (with no cooling), the payback period of the PV system's installation is found equal to 18 years. When considering the PV/t panels, i.e. the panels are air cooled and the extracted thermal energy is used for the desiccant regeneration, the payback period is greatly shortened due to savings on thermal energy and improvement in electricity production, and is found equal to 8 years, which shows the clear advantage of making use of the extracted thermal energy from the panels over the use of PV panels alone.

Conclusion

The PV/t assisted desiccant system was studied for a typical office space in Beirut, Lebanon. The operation was for summer cooling and winter heating, and the simulation was run for the

months of January, April, August and September, and the system's operations was optimized. The system's energy consumption was studied and it was found that thermal energy savings of 85% and 71% can be achieved in winter and summer, respectively. Moreover, electric energy savings of 108% can be reached in April and 119% in summer months due to the high solar irradiance and the improved electrical efficiencies of the panels due to the air cooling. The yearly electricity production is increased by 4% and the investment in the PV/t panels at an interest rate of 4% will result in a payback period of 8 years due to savings on electrical and thermal energies.

Acknowledgment

The financial support of the Munib Masri Institute for Energy and Natural Resources at the American University of Beirut is highly acknowledged.

References

- Beccali, M., R. S. Adhikari, and F. Butera, V. 2004. Franzitta V. Update on desiccant wheel system. *International Journal of Energy Research* 28:1043–49.
- Beccali, M., P. Finocchiaro, and B. Nocke. 2009. Energy and economic assessment of desiccant cooling systems coupled with single glazed air and hybrid PV/thermal solar collectors for applications in hot and humid climate. *Solar Energy* 83:1828–46.
- Bergene, T. and O. Lovik. 1995. Model calculations on a flat-plate solar heat collector with integrated solar cells. *Solar Energy* 55:453–62.
- Dubey, S. and A. A. O. Tay. 2014. The theoretical modelling and optimization of a 10 KWP photovoltaic thermal system for a student hostel in Singapore. *International Journal of Green Energy*. 11(3):225–39.
- El Hourani, M., K. Ghali, and N. Ghaddar. 2014. Effective desiccant dehumidification system with two-stage evaporative cooling for hot and humid climates. *Energy and Buildings* 68:329–38.
- Fanger, P. O. 1982. *Thermal Comfort, Analysis and Applications in Engineering*. New York: McGraw-Hill.
- Garg, H. P., and R. S. Adhikari. 1999. Performance analysis of a hybrid photovoltaic/thermal (PV/T) collector with integrated CPC trough. *International Journal of Energy Research* 23:1295–304.
- Hammoud, M., K. Ghali, and N. Ghaddar. 2014. Optimized operation of solar hybrid desiccant/displacement ventilation combined with personalized evaporative cooler. *International Journal of Green Energy* 11:141–60.
- Hedayatizadeh, M., Y. Ajabshirchi, F. Sarhaddi, A. Safavinejad, S. Farahat, and H. Chaji. 2013. Thermal and electrical assessment of an integrated solar photovoltaic thermal (PV/T) water collector equipped with a compound parabolic concentrator (CPC). *International Journal of Green Energy* 10(5):494–522.
- Hegazy, A. 2000. Comparative study of the performances of four photovoltaic/thermal solar air collectors. *Energy Conversion and Management* 41:861–81.
- HOMER Energy 2.81 ©, HOMER Energy Modeling Software, <http://homerenergy.com/software.html> (2010).
- Hu, H., R. Wang, and G. Fang. 2010. Dynamic characteristics modeling of a hybrid photovoltaic–thermal heat pump system. *International Journal of Green Energy* 7(5):537–51.
- Kinney, L. 2004. New evaporative cooling systems: an emerging solution for homes in hot dry climates with modest cooling loads. *Southwest Energy Efficient Project (SWEET)*.
- Kulkarni, R. K. and S. P. S. Rajput. 2011. Comparative performance of evaporative cooling pads of alternative materials. *International Journal of Advanced Sciences and Technologies* 10 (2):239–44.
- Kumar, R. and M. Rosen. 2011a. Performance evaluation of a double pass PV/T solar air heater with and without fins. *Applied Thermal Engineering* 31:1402–10.

- Kumar, R., and M. Rosen. 2011b. A critical review of photovoltaic-thermal solar collectors for air heating. *Applied Energy* 88:3603–14.
- Mei, L., D. Infield, U. Eicker, and V. Fux. 2003. Thermal modeling of a building with an integrated ventilated PV façade. *Energy and Buildings* 35:605–17.
- Parida, B., S. Iniyar, and R. Goic. 2011. A review of solar photovoltaic technologies. *Renewable and Sustainable Energy Reviews* 15:1625–36.
- Pei, G., T. Zhang, H. Fu, J. Ji, and Y. Su. 2013. An experimental study on a novel heat pipe-type photovoltaic/thermal system with and without a glass cover. *International Journal of Green Energy* 10 (1):72–89.
- Prakash, J. 1994. Transient analysis of a Photovoltaic-thermal solar collector for co-generation of electricity and hot air/water, *Energy Conversion and Management* 35:967–72.
- Ruble, I. and S. Karaki. 2013. Introducing mandatory standards for select household appliances in Lebanon: A cost-benefit analysis. *Energy Policy* 52:608–17.
- Tonoui, J. K. and Y. Tripanagnastopoulos. 2007a. Air-cooled PV/T solar collectors with low cost performance improvements. *Solar Energy* 81:498–511.
- Tonoui, J. K. and Y. Tripanagnastopoulos. 2007b. Improved PV/T solar collectors with heat extraction by forced or natural air circulation. *Renew Energy* 2007; 32:623–37.
- TRNSYS, Transient System Simulation Tool Software. Thermal Energy System Specialists, LLC. Madison Wisconsin, 2010. <http://www.tess-inc.com/>
- Vokas, G., N. Christandonis, and F. Skittides, 2006. Hybrid photovoltaic-thermal systems for domestic heating and cooling—A theoretical approach. *Solar Energy* 80(5):607–13.
- Yassine, B., K. Ghali, N. Ghaddar, I. Srour, and G. Chehab, 2012. A numerical modeling approach to evaluate energy-efficient mechanical ventilation strategies. *Energy and Buildings* 55:618–30.
- Zondag, H. A., D. W. de Vries, W. G. J. van Helden, R. J. C. van Zolingen, and A. A. van Steenhoven. 2003. The yield of different combined PV-thermal collector designs. *Solar Energy* 74:253–69.